Control of Mosaic and Turing Patterns by Light and Electric Field in the Methylene Blue−Sulfide−Oxygen System

M. Watzl and A. F. Münster*

Institut für Physikalische Chemie der Universität Würzburg, Am Hubland, D-97074 Würzburg, Germany

Received: August 21, 1997; In Final Form: February 5, 1998

A variety of spatial patterns emerging in a system containing Methylene Blue, sulfide, and oxygen in a liquid layer and in a polyacrylamide gel are presented. We show the formation of long-lasting mosaic patterns arising from hydrodynamic instability and the transition from an irregular to a more regular, striped structure which occurs under the influence of an external electric field. We also demonstrate the formation of Turing patterns in a gel matrix. Here the gel plays an important role in the pattern formation process by slowing down the diffusion of the activator MB^+. We present experiments showing that pattern formation can be influenced by visible light. An inhomogeneous illumination of the gel-sheet leads to selected regions of activity, which generates stripes instead of hexagons.

Introduction

The formation of spatial patterns induced by the interaction of a nonlinear chemical reaction with transport processes is one of the most interesting phenomena in the field of nonlinear dynamics.[1] Among the variety of transport processes, molecular diffusion plays an important role and the time evolution of different species can be described by reaction−diffusion equations. Target patterns,[2] spiral patterns,[2] and irregular structures[3] have been found in chemical systems in the past decades. In addition, the study of stationary Turing patterns has become of increasing interest in recent years.[4] The spontaneous formation of spatial patterns is, of course, not restricted to chemical systems; in different biological systems, such as the slime mold *Dictyostelium discoideum*,[5] bacteria colonies,[6] and cardiac muscle,[7] comparable phenomena have also been observed.

In his pioneering work A. Turing predicted in 1952 that coupling between reaction and diffusion processes in nonlinear systems can lead to the formation of stationary stable structures.[8] This is of particular interest with respect to biological morphogenesis. However, it took nearly 40 years to obtain such stationary Turing structures in chemical experiments (using the chlorite−iodide−malonic acid reaction[9]), whereas comprehensive theoretical studies were performed in the late 1960s.[10,11] A necessary condition to obtain Turing patterns is a significant difference in the diffusion coefficients of activating and inhibitory species: the activator must diffuse more slowly than the inhibitor, resulting in a local activation and long-range inhibition. A second chemical reaction−diffusion system in which stationary spatial patterns can be realized is the polyacrylamide−Methylene Blue−sulfide−oxygen system (PA-MBO).[12] Turing patterns in this reaction were discovered in our group in 1995, and the experimental system is more convenient to handle than the CIMA reaction.

In this work we present spatial patterns obtained in the Methylene Blue−sulfide−oxygen (MBO) system, and we show the effects of electric field and illumination on them. First we show the formation of long-lasting mosaic patterns in a thin liquid layer resulting from an interaction of a hydrodynamic and a diffusion-induced instability, and then we present stationary structures resulting from a symmetry-breaking instability which are built in a polyacrylamide gel matrix.

Since ionic intermediates are involved in the pattern formation process in most chemical and biological systems, it is interesting to experimentally investigate the influence of an electric field on the observed structures. Until now much work on electric field effects on spatial patterns has focused on the Belousov−Zhabotinsky (BZ) reaction in an excitable system. Studies were performed on pulse waves in quasi one-dimensional systems,[13−17] on spiral waves,[18−23] and on reduction waves.[24] The effects of electric field on the wave propagation velocity together with wave splitting and reversal were demonstrated. The change of spiral wave kinematics and the movement of the spiral tip under the influence of the electric field have been discussed. In the PA-MBO system ionic intermediates are involved, and it allows the study of the effects of an externally applied electric field on mosaic (this work) and Turing patterns.[25] In case of mosaic patterns we observed a reorganization to stripes that are always oriented parallel to the electric field vector, independent of the electric field intensity.

Another external parameter that can be used to influence and control chemical oscillations and pattern formation is light intensity. Several publications deal with the influence of light on oscillations,[26−32] on waves,[33−36] and recently also on spiral waves in the BZ reaction.[37−40] No work has been done to investigate light effects on Turing structures in a light-sensitive system. Considering the homogeneous MBO reaction, illumination causes an increase of the oscillatory frequency in a CSTR with increasing light intensity. Light also controls the Turing pattern formation in the gel matrix.

Characterization of the PA-MBO System

The Methylene Blue−sulfide−oxygen oscillator (MBO) was introduced in the literature by Burger and Field in 1984.[41] The overall chemical reaction consists of the Methylene Blue-catalyzed oxidation of hydrogen sulfide (HS^-) by molecular oxygen in an unbuffered aqueous solution at pH = 10−12. The dye Methylene Blue exists in two stable forms, MB^+ and MBH.

* To whom correspondence should be addressed.

S1089-5639(97)02741-2 CCC: $15.00
Published on Web 03/21/1998

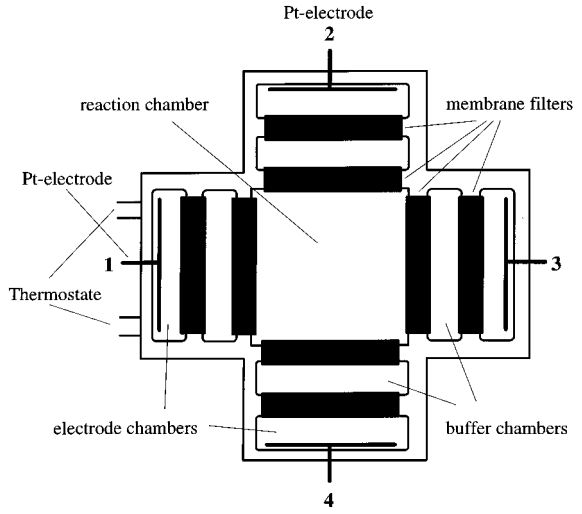

Figure 1. Schematic drawing of the cross-shaped five-chamber reactor used to impose an electrical field onto a thin reaction−diffusion convection layer. The electrode chambers were filled with sodium hydroxide solution of pH (10−12) equal to the reaction mixture. The buffer chambers and the reaction chamber were filled with the reaction mixture. The chambers were connected via membrane filters made from nitrocellulose.

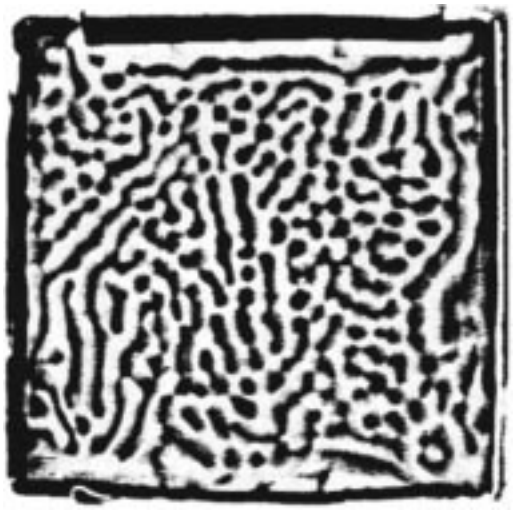

Figure 2. Mixed mosaic pattern of stripes and spots formed by Marangoni convection in a 2 mm solution layer. The dark color corresponds to the oxidized form and the white regions to the reduced form of Methylene Blue. Initial concentrations in the reaction chamber are $[MB^+]_0 = 3.0 \times 10^{-4}$ M, $[Na_2S]_0 = 2.1 \times 10^{-2}$ M, and $[Na_2SO_3]_0 = 1.0 \times 10^{-3}$ M. $T = 22$ °C.

The oxidized form MB^+ is blue colored and has an absorption maximum at 668 nm. The reduced form MBH is colorless. During oscillations in a CSTR MB^+ and MBH are mutually interconverted, while MB^+ is reduced by HS^- and MBH is oxidized by O_2. A reaction mechanism explaining CSTR oscillations has been proposed by Resch et al.[42,43] From a reduced mechanism Zhang et al.[44] conclude that the nonlinearity of the reaction is not a formal autocatalytic step but is caused by a double inhibition of radical chain processes. Molecular oxygen inhibits the reduction of MB^+ to MBH until the catalytically active couple $MB^+/MB^\bullet$ catalyzes the removal of most of the O_2. In the meantime a product of the reduction, $HS^\bullet$, inhibits the reoxidation of MBH to MB^+ until it is removed by O_2, which is provided by exchange with the surrounding atmosphere. Although the nonlinearity of this reaction is not caused by a simple autocatalysis, MB^+ can be considered as "activator": performing a stoichiometric network analysis of the detailed mechanism, it was shown that activation by MB^+ can be interpreted in the sense of a competitive autocatalysis, whereas radical species such as O_2^- and $HS^\bullet$ act as inhibitors.[45]

Experimental Section

Materials. Solutions of purified Na_2S[44] were prepared by dissolving appropriate amounts of recrystallized, water-free Na_2S in N_2-saturated double-distilled water. Other chemicals and reagents of the gel components were used without further purification. Oxygen-containing solutions were prepared by bubbling O_2 until saturation was reached ($\approx 1.2 \times 10^{-3}$ M at 20 °C).

Apparatus and Procedures. All experiments on *hydrodynamic structures* were carried out in a cross-shaped five-chamber reactor (Figure 1). We used this kind of reactor to avoid contamination of the reaction mixture with products of electrode reactions during experiments with an externally applied electric field. To avoid pollution effects by chemical reactions taking place at the electrode surface, the platinum electrodes were immersed in the outer chambers filled with a solution of sodium hydroxide possessing the same pH as the reaction mixture. These electrode chambers were connected to buffer chambers containing the MBO reaction mixture (aqueous solutions of Methylene Blue−chloride-trihydrate, Na_2S, and Na_2SO_3; for concentrations see Figure 2) via membrane filters acting as salt bridges. In the same way, the reaction chamber was connected to the buffer chambers. The size of the electrode chamber and buffer chamber is 15 × 50 × 4 mm (length × width × height), and the reaction chamber size is 50 × 50 × 4 mm. To apply the electric field, the platinum electrodes were connected to a dc power generator (0−60 V). The whole setup was covered with a glass plate, leaving ∼5 mm free space between the fluid surface and the plate, and was thermostated at 22.0 °C. The patterns formed were monitored with a CCD camera.

Our measurements of *Turing structures* were performed in a semibatch gel-reactor, which allows the exchange of oxygen between the gel-matrix and air. Thus the system is open with respect to molecular oxygen but closed with respect to the remaining species. In an experiment we mixed the components of the polyacrylamide gel (aqueous solutions of acrylamide, *N*,*N*′-methylenebisacrylamide, triethanolamine, and ammonium persulfate) with the solutions of the MBO reacting system as outlined in ref 12. This mixture is poured into a thermostated Petri dish (90 mm diameter), resulting in a layer of about 2 mm thickness. The patterns were monitored in transmitted white light using a light box (daylight tubes 2 × 15 W, color temperature 5000 K, 4000 lx) with a CCD camera.

In the experiments under selective illumination the entire Petri dish with all reaction solutions was illuminated during the first 3 min of the polymerization process with the light box described above. To ensure homogeneous illumination, we placed a diffuser plate between the light source and the dish. Using band-pass filters we determined the range of wavelengths efficient for light perturbation to be between 600 and 700 nm. In the following experiments the filters were omitted and selected regions of the gel-sheet were illuminated after the first 3 min with white light from a halogen lamp (12 V/35 W, max. color temperature 3000 K). The lamp was connected to a voltage generator (0−30 V) for adjustable light intensity. Using a convex lens and a deflecting prism, a defined area of nearly homogeneous high illumination was generated on the gel surface. The light intensity distribution was measured with a digital Luxmeter. Using a cover plate placed in front of the

lamp, different geometries of highlighted areas projected onto the gel could be realized. After about 10 min the polymerization process was finished and the halogen lamp could be turned off. Inside the highlighted area the reaction was accelerated compared to the less illuminated surroundings. Therefore the regions of different illumination differ with respect to their initial chemical composition.

All experiments related to homogeneous *oscillations* were carried out in a 1 cm spectrophotometric cell with a volume of 1.28 mL. This CSTR contained a Teflon stirrer, mixing the solutions at 800 rpm, and was fed by two 50 mL gastight syringes via high-precision pumps driven by a stepping motor.[46] The first syringe contained a N_2-saturated 9.37×10^{-2} M Na_2S solution; the second, a 6.0×10^{-6} M MB^+ solution with an O_2 concentration of 1.2×10^{-3} M (O_2-saturated). The cell was thermostated at 21.3 ± 0.1 °C and was placed in a Hewlett-Packard diode array spectrophotometer. The absorption at 668 nm, the absorption maximum of MB^+, was monitored as a function of time. The additional irradiation of the cell resulted from a 12 V/20 W (max. color temperature 3000 K) halogen lamp, focused via a convex lens and located beside the cell; that is, the detection beam of the spectrophotometer and the halogen light beam were oriented perpendicular to each other. We measured the absorption values in intervals of 5 s: the detection beam was interrupted by a shutter for 4.5 s and then directed onto the cell for 0.5 s. Thereby the changes in amplitude and frequency of the observed oscillations were due to the illumination with the halogen lamp, and the effect of the spectrophotometer lamp can be neglected.

Results and Discussion

Mosaic Patterns. In a thin liquid layer of 2 mm thickness we obtained a spatially irregular structure with sharp boundaries that remained almost stationary for about 1 h (Figure 2). After this time the boundaries became more and more diffuse, and finally the solution became homogeneous. The pattern arose about 10 min after mixing the solutions of Methylene Blue, Na_2S, and Na_2SO_3 together. In the figure, the black color indicates regions of high MB^+ concentration.

The observed mixture of spots and stripes was formed by an interaction of surface-tension-driven Marangoni convection and nonlinear reaction and diffusion processes. The MBO reaction consumes oxygen from the air, and the reaction therefore starts at the surface of the liquid. This results in concentration and surface-tension gradients in the plane of the liquid surface. Via hydrodynamic rolls induced by Marangoni convection, oxygen is transported into deeper layers of the solution. In the regions of high O_2 concentration MBH can be oxidized to MB^+, and thus blue-colored mosaic patterns appear. The oxidation is possible only in regions with relatively high O_2 concentration, because MB^+ is reduced by HS^- to MBH at low O_2 concentration.

The following observations confirm the interpretation of pattern formation in terms of Marangoni convection: in a range between 12 and 28 °C the patterns were not sensitive toward temperature; that is, the temperature gradient between dish and air did not alter the patterns. In addition, covering the liquid surface with a glass plate completely suppressed pattern formation even if oxygen-saturated solutions were used; if the surface was covered with a layer of cyclohexane (3 mm), only few convective rolls were formed. Finally, we found a linear relationship between average wavelength and layer depth, which is characteristic for hydrodynamic pattern formation (Figure 3). Similar mosaic patterns have been reported in other nonlinear reactions.[47−54]

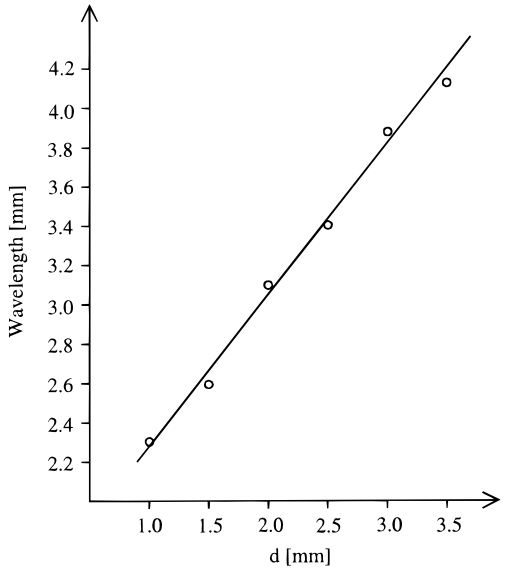

Figure 3. Linear relationship between the pattern wavelength and the thickness (*d*) of the fluid layer.

Turing Patterns. More interesting than these hydrodynamic structures are the patterns formed in a polyacrylamide gel matrix, where convective instabilities can be excluded. After mixing all components of the PA-MBO system, the polymerization of the gel-matrix (under illumination of 4000 lx) is finished after about 10 min and a spatially homogeneous state is observed. After this process, the gel was covered with a thin layer of MB^+ solution (1.0×10^{-4} M) to avoid drying of the surface. From the initially formed homogeneous state different kinds of patterns grow in place after about 30 min, depending on the initial concentrations of Methylene Blue and sulfide. A phase diagram in the plane of initial concentrations was given in ref 12. As an example, a blue hexagonal pattern is shown in Figure 4a. This Turing-type structure is not perfectly stationary in time because we used a semibatch reactor open to oxygen only. Therefore, the chemical reaction tends to reach thermodynamic equilibrium. Nevertheless, the patterns can be monitored for some hours. The black color corresponds to high MB^+ concentration as in Figure 2; the bright regions correspond to the reduced form of the dye MBH. The characteristic wavelength of the pattern is about 2 mm and depends only on intrinsic parameters, e.g., changes in chemical concentrations, temperature, and reaction rates. It does not depend on the geometry of the dish or the layer thickness. The hexagonal symmetry can immediately be seen in a two-dimensional spatial Fourier transform (Figure 4b) which displays six peaks of equal intensity at an angular distance of 60° ± 1°.

A necessary condition for Turing patterns is that the inhibitory species diffuses sufficiently faster than the activating one. In the PA-MBO system, the polyacrylamide gel plays an active role in the pattern formation by decreasing the diffusivity of the activator MB^+. In ref 12 we compared the absorption spectra of MB^+ in liquid and gel phases. Both spectra display an absorption maximum at $\lambda_1 = 668$ nm. The intensity of a second maximum at $\lambda_2 = 616$ nm has been increased in the spectrum measured in the gel phase, however. The second maximum indicates the formation of a dimer MB_2^{2+}. It is known from the literature[55,56] that this dimer is produced in liquid phase at higher concentrations of Methylene Blue ($> 10^{-3}$ M). In the PA matrix the formation of the dimer is enhanced, and thus the diffusivity of MB^+ is reduced. The active role of the polyacrylamide gel for Turing pattern formation in the PA-

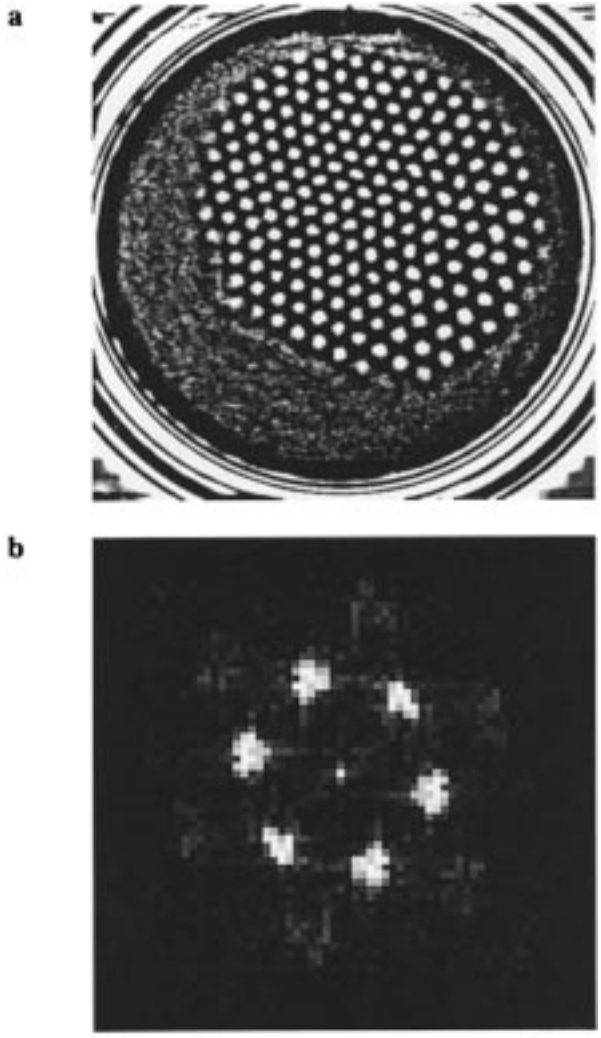

Figure 4. (a) Blue hexagonal Turing pattern in the PA-MBO system. The concentrations inside the gel after mixing are $[MB^+]_0 = 3.97 \times 10^{-4}$ M, $[Na_2S]_0 = 2.54 \times 10^{-2}$ M, and $[Na_2SO_3]_0 = 1.2 \times 10^{-3}$ M. (b) Spatial frequency distribution of the hexagonal pattern in Figure 3a.

MBO system is further supported by the observation that no patterns could be found in experiments with other gels such as agarose or methylcellulose. Other Turing patterns found in this system are blue hexagonal spots, stripes, and zigzag patterns.[12,25]

Effects of Electric Field on Mosaic Patterns. Applying an electric field of 1.5 V/cm $< E <$ 4.0 V/cm in the plane of the liquid layer leads to the formation of stripes oriented parallel to the direction of the electric field vector. In Figure 5a a striped hydrodynamic mosaic pattern formed under the influence of an electric field is shown. The polarity of the electrodes is chosen in the following way: electrode number 1 (see Figure 1) acts as anode (+) and electrode 3 as cathode (−), electrodes 2 and 4 are not used {notation: +, 0, −, 0 ≡ electrode 1 (anode), 2 (neutral), 3 (cathode), 4 (neutral)}. It is now possible to rotate the stripes by changing the polarity of the electrodes. Choosing electrodes 1 and 2 as anodes and electrodes 3 and 4 as cathodes (+, +, −, −) leads to a rotation of the stripes by 45° so that their orientation is again parallel to the electric field vector (Figure 5b). In the vicinity of the walls the stripes are oriented almost perpendicular to the electrodes, indicating the direction of the electric field lines. Another rotation by 45° can be achieved by changing the polarity to (0, +, 0, −) so that the stripes are now perpendicular to the original orientation in Figure 5a. In this way it is possible to rotate the stripes by 360°,

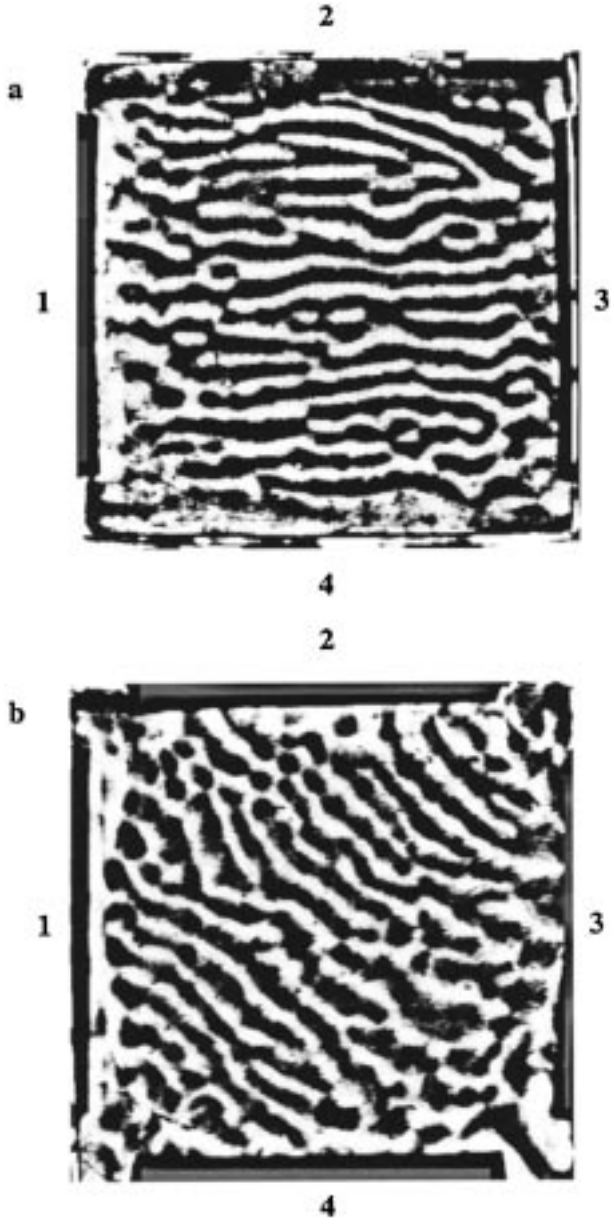

Figure 5. Striped mosaic pattern formed under the influence of electric field: (a) anode at the left (1) and cathode at the right (3) electrode; (b) anode at the left (1) and top (2), cathode at the right (3) and bottom (4) side. The orientation of the stripes is always parallel to the direction of the electric field vector. Conditions are the same as in Figure 2.

cyclically changing the polarity of the electrodes. Adding an excess of a chemically inert electrolyte such as NaCl does not change the behavior. This indicates that the migration of chemically reactive ions—such as MB^+ or O_2^-, which are directly involved in the chemical reactions—is not essential for the observed reorganization of the patterns. The effects are due to convection, which is susceptible to the migration of any ions present in the system. The orientation of the rolls is indicated by the chemical reaction that leads to the formation of blue stripes. The stripes, however, are always oriented parallel to the electric field, independent of the electric field intensity.

In contrast to these observations the effect of the electric field on Turing patterns depends on the intensity of the applied field. Here a weak electric field leads to stripes parallel and a strong field to stripes perpendicular to the electric field vector.[25,57]

Effects of Visible Light on Oscillations and Turing Structures. The behavior of the Methylene Blue−sulfide−oxygen

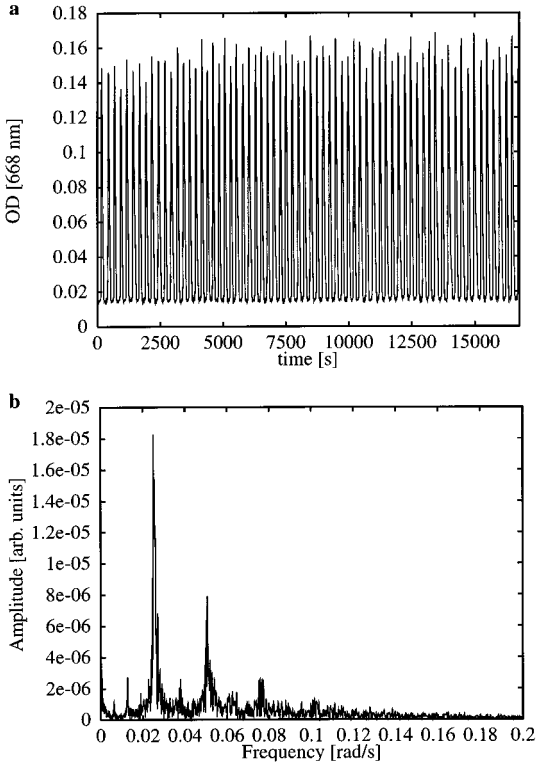

Figure 6. (a) P1 oscillations in a CSTR (absorbance at 668 nm due to MB^+) at 1090 lx. Initial concentrations in the reactor are $[MB^+]_0 = 3.0 \times 10^{-6}$ M, $[Na_2S]_0 = 4.69 \times 10^{-2}$ M, $[O_2]_0 = 6.0 \times 10^{-4}$ M, $T = 21.3$ °C, and $k_f = 2.78 \times 10^{-3}$ s^{-1}. (b) Fourier spectrum of the P1 oscillations of Figure 6a.

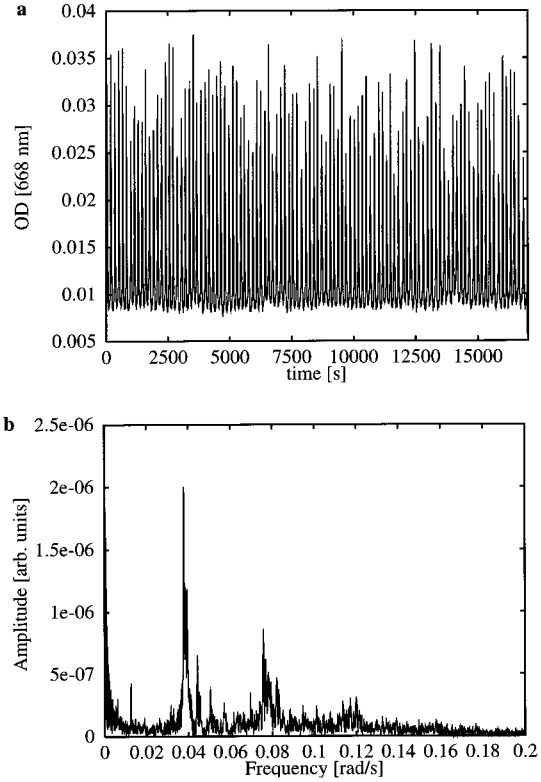

Figure 7. (a) P1 oscillations (absorbance at 668 nm due to MB^+) at 22 000 lx. Conditions are the same as Figure 9a. (b) Fourier spectrum of the P1 oscillations of Figure 7a.

oscillator under CSTR conditions is well-known from experimental and numerical work.[42−44,58] No work, however, has been done to study the effect of light on the oscillations in the MBO. During our examinations of Turing patterns we found that light affected the pattern formation process (described below), and it thus was obvious to study the light effect on oscillations, too.

CSTR experiments. Figure 6a displays period-1 (P1) oscillations at an illumination of 1090 lx, and Figure 6b shows the corresponding Fourier spectrum. Increasing the light intensity to 22 000 lx results in an increased frequency of the P1 oscillations. Figure 7a,b displays the measured time series and the corresponding Fourier spectra at 22 000 lx. The frequency of oscillations increases from $\nu_{1090} = 2.51 \times 10^{-2}$ rad/s to $\nu_{22000} = 3.79 \times 10^{-2}$ rad/s at higher illumination intensity. With increasing light intensity, the amplitude of oscillations and the signal-to-noise ratio decrease until the oscillations vanish at illumination above 40 000 lx. It is known from the literature that a reactive triplet (T1)-state MB^{+*} is the reactive species during the reduction of MB^+ to MBH by a reducing agent, e.g. Fe^{2+}.[59,60] In the MBO reaction hydrogen sulfide ions play the role of the reducing agent. The triplet state is formed by light absorption at 668 nm, and thus the reactivity of Methylene Blue toward reducing agents can be controlled. At higher illumination intensity the reactive triplet state is populated more rapidly, and the reaction rate of the reduction of MB^+ and the oscillatory frequency increase. Figure 8 displays the relation between illumination intensity and the frequency of CSTR oscillations. To clarify the influence of light intensity on the oscillations, we studied the photosensitive reduction of MB^+ by sulfide under exclusion of O_2 in a spectrophotometric cell. The overall rate law of this reaction is given in eq 1.[43]

$$-\frac{d[MB^+]}{dt} = k_i[MB^+]^{0.5}[HS^-]^{1.5} \quad (1)$$

This rate equation results from the following radical-chain mechanism:[43]

$$MB^+ + HS^- \rightarrow MB^\bullet + HS^\bullet \quad (2)$$

$$H_2O + MB^\bullet + HS^- \rightarrow MBH + HS^\bullet + HO^- \quad (3)$$

$$HO^- + HS^\bullet + MB^+ \rightarrow MB^\bullet + S + H_2O \quad (4)$$

$$H_2O + MB^\bullet + MB^\bullet \rightarrow MB^+ + MBH + HO^- \quad (5)$$

We measured the absorption−time curves (668 nm) of MB^+ in this reaction cascade under oxygen exclusion and under increasing illumination. Figure 9 displays the obtained absorption curves. With increasing light intensity MB^+ is reduced faster to MBH. From the curves we computed the reaction rate constants k_i of eq 1 assuming an excess and therefore a constant HS^--concentration. The rate constant k_i increases from $k_0 = 2.2 \times 10^{-3}$ $M^{-1}s^{-1}$ at no external illumination to $k_{6800} = 3.8 \times 10^{-3}$ $M^{-1}s^{-1}$ at 6800 lx to $k_{22000} = 6.1 \times 10^{-3}$ $M^{-1}s^{-1}$ at 22000 lx, and finally to $k_{64000} = 9.3 \times 10^{-3}$ $M^{-1}s^{-1}$ at 64000 lx. The reaction rate therefore is accelerated by increasing illumination. To compare the experimental results with numerical simulations we used the MBO mechanism described by Resch et al.[43] In their mechanism reaction 2 of the reaction cascade is assumed to have a rate constant of $k_{(2)} = 0.1$ $M^{-1}s^{-1}$. We assume that the effect of illumination on this particular reaction results in an increased reaction rate and that the main contribution to the overall illumination effects is made by this reaction. Computations using $k_{(2)} = 0.1$ $M^{-1}s^{-1}$ displayed regular P1 oscillations, depicted by the dashed line in Figure 10. Increasing the rate

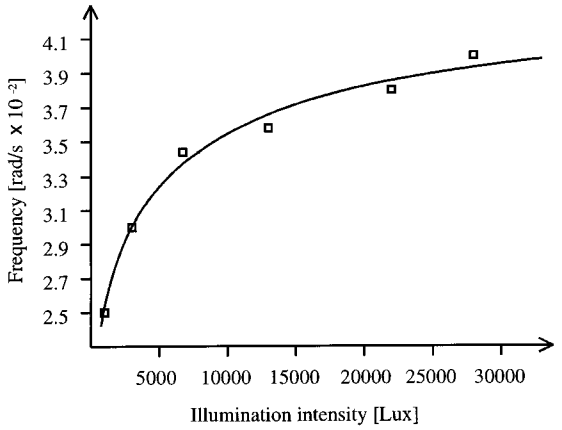

Figure 8. Relation between illumination intensity and the frequency of the CSTR oscillations. At an illumination intensity above 40 000 lx the oscillations are quenched.

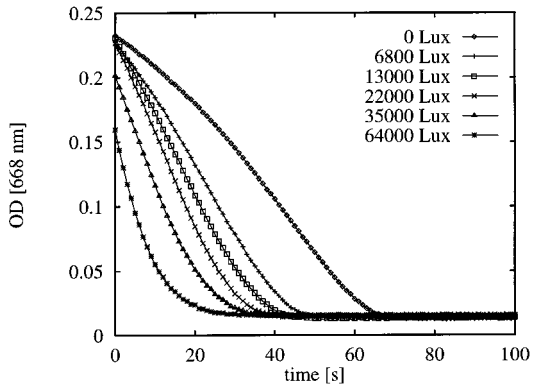

Figure 9. Absorption−time curves due to the absorbance of MB^+ during the reduction of MB^+ by sulfide under oxygen exclusion (reactions 2−5) with external illumination intensities from 0 to 64 000 lx.

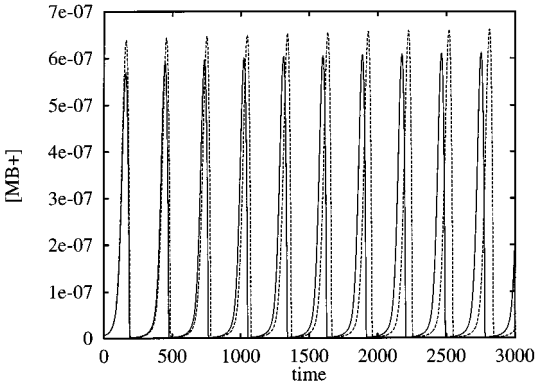

Figure 10. Computed P1 oscillations at different reaction rates $k_{(2)}$ of the reaction $MB^+ + HS^- \rightarrow MB^\bullet + HS^\bullet$ (2). $k_{(2)} = 1.0\ M^{-1}s^{-1}$ (solid line) and $k_{(2)} = 0.1\ M^{-1}s^{-1}$ (dashed line).

constant $k_{(2)}$ by a factor of 10, without changing any other parameter, led to oscillations depicted by the solid line in Figure 10. The frequency of the oscillations has been increased and the amplitude is smaller at the higher rate constant. Although the computed effects are small, the direction of frequency and amplitude changes is qualitatively reproduced by the model.

Experiments in the PA Gel. The Turing patterns formed in the gel matrix also depend on illumination. If the illumination of the gel-sheet is too weak, the reduction of MB^+ is so slow that pattern formation requires several hours. On the other hand, if the illumination is too strong, pattern formation is suppressed by increasing the reduction rate of MB^+. The system now

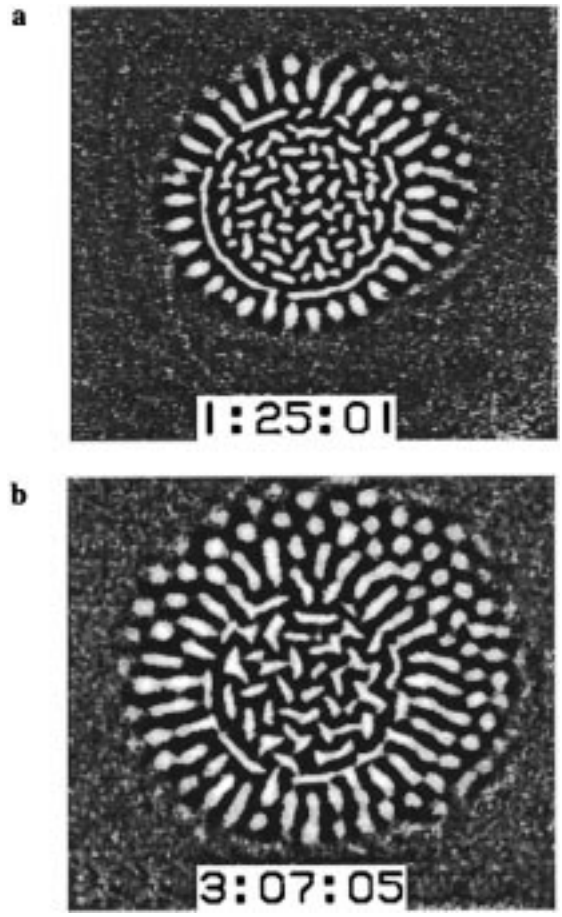

Figure 11. Turing pattern formed under inhomogeneous illumination. A circular area of 20 mm diameter was illuminated with 22 000 lx, whereas the surrounding area was illuminated with 3900 lx. (a) Snapshot taken 1 h 25 min 1 s after mixing the reagents; (b) snapshot of the same region after 3 h 7 min 5 s.

remains in its reduced state. Between these two extreme cases pattern formation can be affected by selective illumination of the reaction−diffusion system. Figure 11a,b displays a pattern formed under conditions where a circular area of 20 mm diameter in the gel was illuminated at an intensity of 22 000 lx, whereas the surrounding area was illuminated with 3900 lx. The difference between 11a and 11b is when the snapshots were taken. Due to the illumination, the concentration of the reactive triplet state $MB^{+}*$ (T1), during the initial phase of pattern formation, is higher inside the circular area than in the surrounding area. After the halogen lamp was switched off, the highlighted and surrounding areas differ in their chemical compositions. Thus, a diffusive flux is established between bright and dark areas leading to Dirichlet-type boundaries between them. At the border of the different illuminations, stripes start to emerge perpendicular to the borderline (Figure 11a). During the experiment the stripes grow until they reach a particular distance from the borderline and finally break up. According to the intrinsic wavelength of Turing patterns, this scenario is comprehensive: the characteristic wavelength of the stripes is about 2 mm, and the wavelength would have to increase due to the geometric constraint if the stripes grew further. In Figure 11b the breakup and formation of a hexagonal pattern is shown. To obtain longer stripes, it is necessary to create straight lines at the boundary of strongly and weakly illuminated areas. This can easily be realized by changing the geometry of the highlighted area, as shown in Figure 12. Here two parallel rectangular areas were illuminated with high

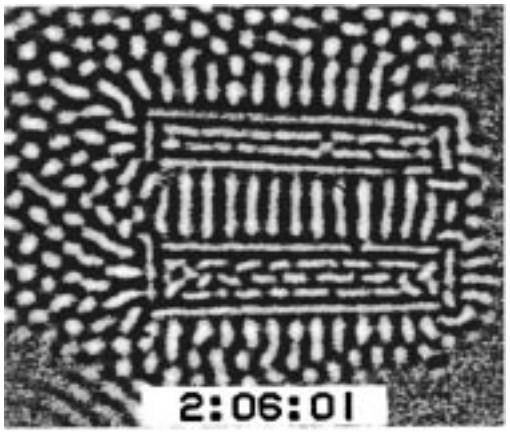

Figure 12. Regular stripes in the PA-MBO system formed between two rectangular highlighted areas (22 000 lx) after 2 h 6 min 1 s.

intensity, and regular stripes grew in the region between them. The bright-to-dark borderlines were characterized by Dirichlet-type boundary conditions, whereas the remaining borders display von Neumann conditions. These experiments show the controlled formation of striped Turing patterns, and they are in agreement with numerical predictions made by Münster et al.[57] in the Brusselator. In that paper we show the formation of striped Turing patterns in a quadratic reaction−diffusion system with mixed boundary conditions.

Conclusion

In this work we present spatial patterns found in a system containing Methylene Blue, sulfide, and oxygen in liquid phase and in polyacrylamide gel. We show the formation of long-lasting mosaic patterns that are generated through hydrodynamic instabilities. The transition from an irregular to a more regular, striped structure under the influence of external electric field is described. The orientation of the stripes is always in the direction of the electric field vector, independent of the field intensity. We also show the formation of Turing patterns in a gel-matrix, where the gel plays an important role in the pattern formation process by decreasing the diffusion coefficient of the activator MB^+. By properly designed illumination of the gel-sheet different regions of activity and different boundary conditions can be realized. This leads to the formation of stripes instead of hexagons. In the PA-MBO system a spatially periodic perturbation of Turing patterns can thus be realized experimentally. The illumination intensity influences the oscillation frequency in a continuous flow stirred tank reactor. With increasing light intensity we found an increasing oscillation frequency and finally a suppression of oscillations.

Acknowledgment. We thank the Deutsche Forschungsgemeinschaft for financial support. We further thank F. W. Schneider, M. Marek, D. Šnita, and M. Eiswirth for helpful discussions

References and Notes

(1) Meinhardt, H. *Models of Biological Pattern Formation*; Academic Press: London, 1982.
(2) Field, R. J., Burger, M., Eds. *Oscillations and Travelling Waves in Chemical Systems*; Wiley-Inerscience: New York, 1985.
(3) Quyang, Q.; Swinney, H. L. *Chaos* **1991**, *1*, 411.
(4) Kapral, R., Showalter, K., Eds. *Chemical Waves and Patterns*; Kluwer Academic Publishers: Dordrecht, 1995.
(5) Gerisch, G. *Naturwissenschaften* **1971**, *58*, 430.
(6) Tsimring, L.; Levine, H.; Aranson, I.; Ben-Jacob, E.; Cohen, I.; Shochet, O.; Reynolds, W. *Phys. Rev. Lett.* **1995**, *75*, 1859.
(7) Davidenko, J.; Kent, P.; Jalife, J. *Physica D* **1991**, *49*, 182.
(8) Turing, A. M. *Philos. Trans. R. Soc. London* **1952**, *237*, 37.
(9) Castets, V.; Dulos, E.; Boissonade, J.; DeKepper, P. *Phys. Rev. Lett.* **1990**, *64*, 2953.
(10) Prigogine, I.; Nicolis, G. *J. Chem. Phys.* **1967**, *46*, 3542.
(11) Prigogine, I.; Lefever, R. *J. Chem. Phys.* **1968**, *48*, 1695.
(12) Watzl, M.; Münster, A. F. *Chem. Phys. Lett.* **1995**, *242*, 273.
(13) Ševcíková, H., Marek, M. *Physica D* **1992**, *9*, 140.
(14) Ševcíková, H.; Marek, M.; Müller, S. C. *Science* **1992**, *257*, 951.
(15) Schmidt, S.; Ortoleva, P. *J. Chem. Phys.* **1981**, *84*, 4488.
(16) Kondepudi, D. K.; Prigogine, I. *Physica A* **1981,** *107*, 1.
(17) Ortoleva, P. *Physica D* **1984**, *26*, 67.
(18) Schütze, J.; Steinbock, O.; Müller, S. C. *Nature* **1992**, *356*, 45.
(19) Steinbock, O.; Schütze, J.; Müller, S. C. *Phys. Rev. Lett.* **1992**, *68*, 248.
(20) Agladze, K. I.; DeKepper, P. *J. Phys. Chem.* **1992**, *96*, 5239.
(21) Pérez-Muñuzuri, V.; Aliev, R.; Vasiev, B.; Pérez-Villar, V.; Krinsky, V. I. *Nature* **1991**, *353*, 740.
(22) Pérez-Muñuzuri, V.; Gomez-Gesteira, M.; Pérez-Villar, V. *Physica D* **1993**, *64*, 420.
(23) Taboada, J. J.; Muñuzuri, A. P.; Pérez-Muñuzuri, V.; Gomez-Gesteira, M.; Pérez-Villar, V. *Chaos* **1994**, *4*, 519.
(24) Kaštánek, P.; Kosek, J.; Šnita, D.; Schreiber, I.; Marek, M. *Physica D* **1995**, *84*, 79.
(25) Münster, A. F.; Watzl, M.; Schneider, F. W. *Phys. Scr.* **1996**, *T67*, 58.
(26) Sharma, K. R.; Noyes, R. M. *J. Am. Chem. Soc.* **1975**, *97*, 202.
(27) Busse, H.; Hess, B. *Nature* **1973**, *244*, 203.
(28) Gáspár, V.; Basza, G.; Beck, M. T. *Z. Phys. Chem.* **1983**, *264*, 43.
(29) Dulos, E.; DeKepper, P. *Biophys. Chem.* **1983**, *18*, 211.
(30) Vanag, V. K.; Alfimov, M. V. *J. Phys. Chem.* **1993**, *97*, 1878.
(31) Jinguji, M.; Ishihara, M.; Nakazawa, T. *J. Phys. Chem.* **1992**, *96*, 4279.
(32) Srivastava, P. K.; Mori, Y.; Hanazaki, I. *Chem. Phys. Lett.* **1992**, *190*, 279.
(33) Kuhnert, L. *Naturwissensch.* **1986**, *73*, 96.
(34) Kuhnert, L.; Agladze, K. I.; Krinsky, V. I. *Nature* **1989**, *337*, 244.
(35) RamReddy, M. K.; Nagy-Ungvarai, Zs.; Müller, S. C. *J. Phys. Chem.* **1994**, *98*, 12255.
(36) RamReddy, M.K.; Dahlem, ;., Zykov, V. S.; Müller, S. C. *Chem. Phys. Lett.* **1995**, *236*, 111.
(37) Steinbock, O.; Müller, S. C. *Int. J. Bif. Chaos* **1993**, *3*, 437.
(38) Steinbock, O.; Müller, S. C. *Physica A* **1992**, *188*, 61.
(39) Steinbock, O.; Zykov, V. S.; Müller, S. C. *Nature* **1993**, *366*, 322.
(40) Grill, S.; Zykov, V. S.; Müller, S. C. *Phys. Rev. Lett.* **1995**, *75*, 3368.
(41) Burger, M.; Field, R. J. *Nature* **1984**, *307*, 720.
(42) Resch, P.; Field, R. J.; Schneider, F. W. *J. Phys. Chem.* **1989**, *93*, 2783.
(43) Resch, P.; Field, R. J.; Schneider, F. W.; Burger, M. *J. Phys. Chem.* **1989**, *93*, 8181.
(44) Zhang, Y. X.; Field, R. J. *J. Phys. Chem.* **1991**, *95*, 723.
(45) Eiswirth, M.; Münster, A. F. To be published.
(46) Schneider, F. W.; Münster, A. F. *J. Phys. Chem.* **1991**, *95*, 2130.
(47) Zhabotinsky, A. M.; Zaikin, A. N. *J. Theor. Biol.* **1973**, *40*, 45.
(48) Orban, M. *J. Am. Chem. Soc.* **1980**, *102*, 4311.
(49) Showalter, K. *J. Chem. Phys.* **1980**, *73*, 3735.
(50) Strizhak, P. E. *Chem. Phys. Lett.* **1995**, *241*, 360.
(51) Micheau, J. C.; Gimenez, M.; Borckmans P.; Dewel, G. *Nature* **1983**, *305*, 43.
(52) Avnir, D.; Kagan, M. *Nature* **1984**, *307*, 717.
(53) Avnir, D.; Kagan, M. *Chaos* **1995**, *5*, 589.
(54) Rodriguez, J.; Vidal, J. *J. Phys. Chem.* **1989**, *93*, 2737.
(55) Rabinowitch, E.; Epstein, L. F. *J. Am. Chem. Soc.* **1941**, *63*, 69.
(56) Michaelis, L.; Granick, S. *J. Am. Chem. Soc.* **1945**, *67*, 1215.
(57) Münster, A. F., Hasal, P., Šnita, D.; Marek, M. *Phys. Rev. E* **1994**, *50*, 546.
(58) Resch, P.; Münster, A. F.; Schneider, F. W. *J. Phys. Chem.* **1991**, *95*, 6720.
(59) Parker, C. A. *J. Phys. Chem.* **1959**, *63*, 26.
(60) Oster, G.; Wotherspoon, N. *J. Am. Chem. Soc.* **1957**, *70*, 4836.